VOL. 19, NO. 14, JULY 2024 ISSN 1819-6608
ARPN Journal of Engineering and Applied Sciences

www.arpnjournals.com

ADVANCED DEEP LEARNING MODELS FOR COMPREHENSIVE ANALYSIS AND OPTIMIZATION OF NUCLEATE BOILING HEAT TRANSFER SYSTEMS

Mohammad Saraireh, Falah Al-Saraireh and Yassin Nimir
Department of Mechanical Engineering, Faculty of Engineering, Mutah University, Karak, Jordan
E-Mail: maqsaraireh@mutah.edu.jo

ABSTRACT

For heat transfer systems used in nucleate boiling, deep learning-based solutions are required. This is a vital step to avoid the limitations of observational and experimental data. This study aims to combine Generative Adversarial Networks (GANs), Convolutional Neural Networks (CNNs), and Recurrent Neural Networks (RNNs) to enhance computational fluid dynamics (CFD) design. Better designs, such as Visual Geometry Group (VGG16), can extract hierarchical features, while CNNs can distinguish dynamic events such as bubble formation and growth in response to temperature changes. Because it uses current data, this strategy does not require large datasets. Images are processed to recover bubble statistics and physical data using mask R-CNN and other advanced object identification techniques. This approach ties bubble activity to heat flow parameters, resulting in a consistent sample for examination. To better understand boiling processes, the research suggests a dual method. This approach uses CNNs for feature extraction and Multi-Layer Perceptron (MLP) networks for data processing. This technique produces deep learning models and robust optimization tools while also advancing our knowledge of nucleate boiling. In the experimental setup, pool boiling is investigated using one of the precisely constructed heating tanks. This tank enables us to maintain consistent heat transfer when photographing with high-speed cameras. More improved imaging techniques are required for precise observations and analysis, as high-speed camera images demonstrate how minor variations in heat flow can impact bubble dynamics. The whole process of developing, training, and testing deep learning models includes refining data, segmenting instances using Mask R-CNN, and generating hybrid features by merging Mask R-CNN with CNN (VGG16). This strategy may lead to the creation of a regression model capable of reliably predicting heat flow in boiling water tests. The goal is to make the model easier to use and understand. It appears that the study of heat flow prediction and boiling dynamics covered a lot of ground. The average bubble size increases linearly from 0.5 to 5.0 mm when the heat flow increases from 10 to 100 kW/m^2. This suggests an increase in heat flow. When bigger heat fluxes are present, the standard deviation increases, showing that bubble diameters might vary significantly. The recommended deep learning models proved to be very predictive. This study has greatly improved our knowledge and use of nucleate-boiling heat transport systems. The findings show that deep learning models may incorporate theoretical and practical components, resulting in more dependable and efficient thermal management systems.

Keywords: nucleate boiling, heat transfer coefficient, deep learning, computational fluid dynamics, critical heat flux, thermal management.

Manuscript Received 23 May 2024; Revised 3 August 2024; Published 12 October 2024

1. INTRODUCTION

Thermal management and energy systems need effective heat transfer, particularly for accurate temperature control under changing loads. Nucleate boiling is one of the finest techniques to transmit large quantities of heat with minimal temperature variation. The formation of gas bubbles at precise nucleation locations on a heated surface is significant in many disciplines, including power, electronics cooling, and chemical handling. Nucleate boiling is being studied to enhance and extend the lifetime of heat transfer systems because it is efficient and excellent at thermal loads. Several industrial applications employ nucleate-boiling heat transfer devices [1]. Heat energy management affects power plants, electronics, and solar performance, longevity, and efficiency. Understanding and improving these systems has always relied on empirical models and data. Due to their inability to demonstrate how phase transition, fluid dynamics, and heat transfer interact at the micro and nanoscales, these approaches are informative but frequently fail to portray the intricate dynamics of the boiling process [2]. Computing fluid dynamics (CFD) enhanced the heating process model accuracy, advancing the field. CFD is expensive, time-consuming, and cannot be scaled up or changed since it demands a lot of mathematics and exact physical modeling parameters. Deep learning has transformed nucleate boiling event research and improvement. Deep learning can analyze large amounts of data, identify hidden patterns, and generate accurate predictions without physical laws. CNNs, RNNs, and GANs allow us to study and enhance nucleate boiling systems in ways that prior models could not [3]. Nucleate boiling analysis creates data-driven models using deep learning. This model finds complicated, non-linear interactions that other approaches overlook. Data-driven models organize better. They choose optimal neural network parameters [4] for accurate predictions. Data-driven methods may speed up heating, discover the

ideal system settings, and set up control measures. This work analyzes and improves nucleate-boiling heat transfer systems using deep learning. The framework uses predictive modeling to calculate the critical heat flux (CHF) and heat transfer coefficient (HTC). System design optimization and real-time adaptive thermal management control techniques are also included [5]. High-fidelity deep learning models increase heating device performance and efficiency completely. The paper includes significant advances, including the development of high-fidelity deep learning models that properly represent nucleate boiling physics, surpassing earlier observational and numerical models. Optimization technique using deep learning predictions and complex mathematics finds the optimum system parameters [6]. Basic Insights The research helps us comprehend nucleate boiling by providing fresh information. Deep learning models provide real-time control approaches for dynamic control systems, making them more adaptable and efficient. The research indicates that the models and approaches may be applied to numerous levels and systems. They are adaptable and extensively applicable. Advances in deep learning have enhanced nucleate boiling heat transfer system research. This research bridges academic and practical principles. It enables temperature control system advancement [7]. This study increases heating system performance and efficiency and enables greener energy and process engineering solutions [8]. Deep learning may drastically revolutionize thermal system optimization.

Table-1 contains experimental data from investigations on circular mini-channels, which are crucial to nucleate boiling heat transfer systems. Each item discusses distinct testing settings, including saturation pressure, interior diameter, mass flow, heat flux, and refrigerants. These circumstances demonstrate the many parameters that impact nucleate boiling [9]. Based on this data, modern computing and analytic approaches like deep learning are being used to comprehend nucleate boiling. The field uses many complex experimental setups, as seen in this table. It reveals how difficult typical methods are to comprehend nucleate boiling dynamics. Although observational and experimental approaches are crucial, they don't always work well for understanding complicated micro and nanoscale phenomena, including phase change, fluid dynamics, and heat transport [10]. Progress was made using computational fluid dynamics (CFD). It provided greater detail but needed a lot of computational power and precise physical modeling. Recent breakthroughs in deep learning have changed how nucleate boiling events are investigated and improved. These trials generate massive volumes of data, which deep learning models like CNNs, RNNs, and GANs may help us understand [11]. Traditional approaches cannot identify complex, non-linear patterns and correlations, as these models can by learning directly from data. Adjusting neural network parameters reduces prediction errors without using physical laws. Making progress Deep learning offers this. This data-driven approach helps us understand the heating process and determine the optimal system configurations and control techniques for performance. Researchers established a platform to examine and enhance nucleate boiling heat transfer systems using accurate deep learning models [12]. The critical heat flux (CHF) and heat transfer coefficient may be accurately calculated via predictive modeling. It also improves system design and implements real-time temperature management control systems. This table classifies data by physical features crucial for deep learning investigations in systems that transport heat from nucleate boils. Each trait's greatest, lowest, and average figures are shown. These are crucial for forecasting.

Table-1. Summary of experimental conditions from various studies on circular mini-channels in nucleate boiling heat transfer research.

Source	Saturation Pressure (MPa)	Inside Diameter (mm)	Mass Flux (kg/(m²·s))	Heat Flux (kW/m²)	Refrigerant
Wambsganss *et al*. [9]	0.13-0.16	2.92	50 - 300	8.8 - 908	R-113
Tran *et al*. [10]	(55-62)	2.46	66.3 - 300	7.5 - 59.4	R-12
Kew and Cornwell [11]	(34)	1.95	167 - 560	15.6	R-141b
Bao *et al*. [12]	0.83	1.95	167 - 452	12 - 29	R-11
Kuwahara *et al*. [13]	(32)	0.84	525	30 - 50	R-123
Saitoh *et al*. [14]	0.10	0.51, 1-	300 - 1000	6-24	R-134a
Yamashita *et al*. [15]	0.29 - 0.47	1.02	100 - 400	6-24	R-134a
Li *et al*. [8]	(57 - 76)	2.00	100	2-24	CO_2
Enoki *et al*. [4]	0.88	2.00	300	20	R-32
Yokoyama *et al*. [17]	(35)	1.00	200	10	R-1234yf
Wu *et al*. [18]	(10)	1.00	-	20	R-410A
Longo *et al*. [19]	(14)	2.00	-	72	NH3

Table-2 lists several physical properties required to research and enhance nucleate boiling heat transfer systems using deep learning. The Prandtl number, vapor-to-liquid density ratio [13], critical pressure and temperature, specific heat, densities, surface tension, latent heat, viscosities, and others are examples. This table provides each characteristic's greatest, lowest, and average figures. This idea helps deep learning models comprehend nucleate boiling. Knowing this is crucial since nucleate boiling processes are complex and vary with fluid and operation. Every physical characteristic impacts fluid temperature, speed, bubble formation, growth, and breakoff. Beyond the critical temperature and pressure in thermodynamics, liquid and gas cannot be distinguished [14]. Temperature and partial pressure might indicate the boiling point. These factors impact a material's heat capacity, storage, movement, and conductivity. Phase shift requires latent heat; while surface tension helps bubbles develop and remain stable, improving heat transmission. Viscosity, diffusivity, and Prandtl number affect fluid speed and energy. Deep learning algorithms employ several physical properties to discover patterns and relationships in nucleate boils. By training on datasets with these features [15], these models may be able to predict new circumstances, improve system designs, and provide real-time adaptive heat management control. The best, worst, and average data help us make sense of everything and create models that operate well, are versatile, and can be utilized in various situations. This strategy outperforms number-based and observational techniques. It clarifies nucleate boiling processes, making heat control systems last longer and operate better.

Table-2. Deep learning analysis of nucleate boiling physical properties.

Property	Max	Min	Average
Saturation Pressure (MPa)	5.00	0.10	0.90
Vapor Conductivity (W/m·K)	27.32	9.82	14.40
Critical Pressure (MPa)	11.33	3.38	5.34
Liquid Conductivity (W/m·K)	559.20	62.26	142.43
Critical Temperature (K)	487.21	304.13	392.14
Specific Heat at Constant Pressure, C_p (J/kg·K)	4616.54	918.02	1841.10
Vapor Density (kg/m³)	156.67	3.46	33.67
Specific Heat at Constant Volume, C_v (J/kg·K)	2800.29	610.63	1068.92
Liquid Density (kg/m³)	1492.63	638.57	1125.24
Surface Tension (mN/m)	26.30	2.07	11.23
Ratio of Vapor-to-Liquid Density	189.3×10^3	3.97×10^3	32.1×10^3
Latent Heat (kJ/kg)	1262.24	133.73	316.18
Vapor Viscosity (μPa·s)	16.81	9.06	11.75
Diffusivity (m²/s)	18.97×10^{-8}	-	-
Liquid Viscosity (mPa·s)	469.23	75.6	-
Prandtl Number	6.71	3.10	-

2. PROPOSED METHOD

Nucleate-boiling heat transfer systems need a deep learning-based, complicated structure to overcome observational and experimental constraints. This strategy advances understanding and improving these complex systems. CNNs, RNNs, and GANs improve their CFD-based design. CNNs can differentiate fundamental shapes and colors as well as dynamic phenomena like bubble formation and development as temperature changes using hierarchical feature extraction [16]. Thanks to updated deep CNN architectures, such as VGG16, the model may learn from previously gathered data, eliminating the need for large datasets. The algorithm can discover and analyze visual elements that a human would miss while saving time and money on data processing. Mask, R-CNN, and other complicated object recognition algorithms collect bubble statistics and other physical data from images [17-19]. This method saves time and produces a consistent sample for analysis. Nucleate boiling, bubble behavior, and heat flow are linked. MLP neural networks may change feature weights and bubble counts to comprehend boiling. CNNs extract characteristics, but MLP networks train them, helping us comprehend boiling [20-22]. This two-part strategy employs CNNs for hierarchical feature extraction and MLP networks for data processing to demonstrate how deep learning may explain nucleate boiling. Benefits of the research include reliable deep learning models optimization tools and novel nucleate boiling information. This study improves heating systems and sets the framework for temperature control technology advances [23]. The research uses sophisticated deep learning methods to blend theory and practice and provide

scalable solutions for a variety of industrial contexts. This advances nucleate-boiling heat transfer systems significantly.

Figure-1 depicts the pool heating tank's construction and operation throughout all testing. A set thermal connection transmits heat uniformly, a set image distance maintains image size and focus, and a basic copper basis for all tests ensures level surface contacts. This strategy links heating changes to the test setting, not the tools [24]. To compare heat flow data and study copper surface bubbles, the setup must be consistent.

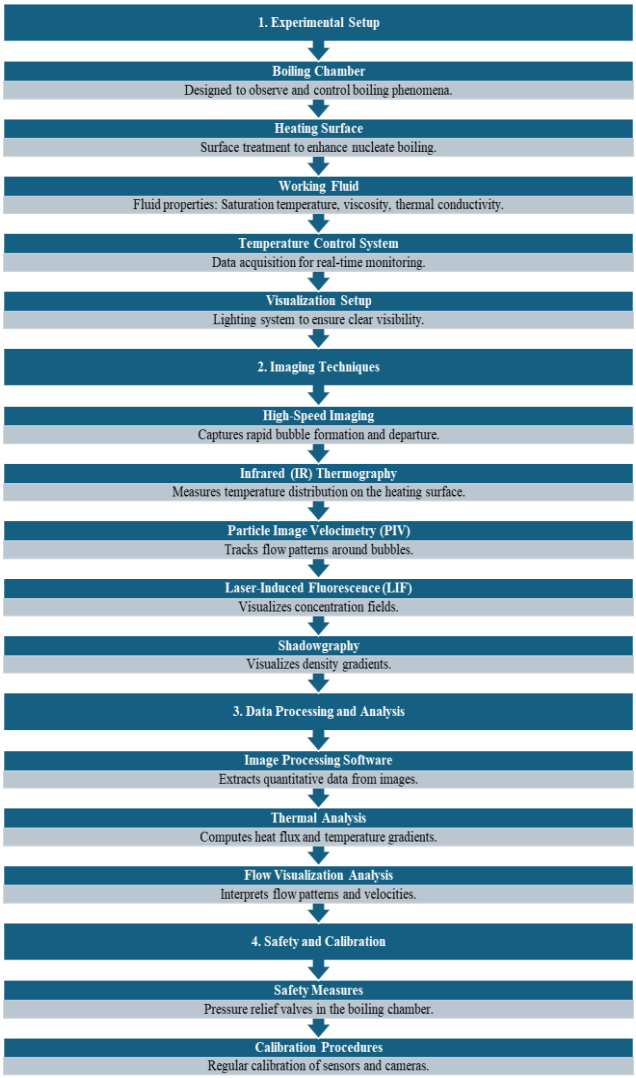

Figure-1. Experimental setup and imaging techniques for pool boiling analysis.

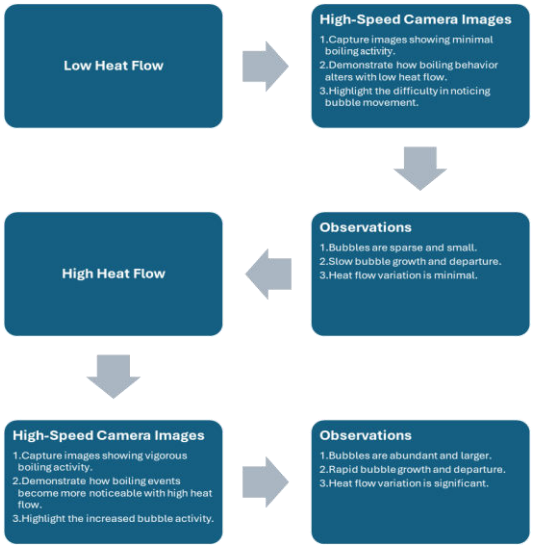

Figure-2. The flow diagram of a high-speed camera shows how boiling behavior may alter.

Time-based bubbles recorded by high-speed cameras reveal how sensitive bubble dynamics may be to modest heat flow changes. Even if the camera is quick and clear, it's impossible to detect how heat fluxes affect bubbles. Figure-2 demonstrates how heat flow alters bubble size, quantity, and form. This capacity to detect changes helps us understand how heat flow impacts bubble movement and boiling at various temperatures. The flow diagram illustrates the importance of understanding nucleate boiling at low and high heat flow. The photographs and notes explain how difficult it is to quantify and record bubble motions in boiling pool research. They emphasize that nucleate-boil heat transfer requires improved imaging and careful experiment control. A CNN model for visual analysis is constructed and improved using this strategy. Set up, train (forward pass, activation, pooling, and loss calculations), test, and release after backpropagation to modify weight. Equations for convolution, activation functions, loss computation, and weight updating help explain CNNs.

Algorithm 1:

1. Initialize weights (W) and biases (b):

$$W = rand(n, m), b = rand(n, 1), W' = rand(k, j) \quad (1)$$

2. Select activation function:

$$f(x) = 1/(1 + e^{-x}),\ g(x) = \max(0, x) \quad (2)$$

3. Load image dataset
4. Normalize images:

$$x' = (x - \mu)/\sigma \quad (3)$$

Where: σ is the standard deviation and μ is the mean

5. Convolution operation for feature extraction:

$$f(x,y) * g(x,y), h(x,y) * k(x,y) \quad (4)$$

6. Apply non-linearity (Rectified Linear Unit (ReLU)):

$$g(x) = \max(0,x), h(x) = x * (x > 0),$$

$$i(x) = \log(1 + e^x) \quad (5)$$

7. Implement pooling to reduce dimensionality.
8. Flatten feature map for fully connected layer:

$$F = flatten(P), G = F * W' + b', H = \sigma(G) \quad (6)$$

9. Apply dropout to prevent overfitting
10. Define loss function (Cross-entropy):

$$L = -\frac{1}{N}[\sum_1^N ylog(\hat{y}) + (1-y)\log(1-\hat{y})] \quad (7)$$

Where: L is average cross-entropy, and N is data points

11. Backpropagation to compute gradients:

$$\frac{\partial w}{\partial L} = \frac{1}{N}(\sigma(XW+b) - Y)^T X, \frac{\partial b}{\partial L} = \frac{1}{N}\sum(\sigma(XW+b) - Y), \frac{\partial W'}{\partial L} = (\sigma(XW'+b') - Y)^T F \quad (8)$$

12. Update weights and biases using gradient descent
13. Evaluate the model on the validation set
14. Adjust hyperparameters (learning rate η, epochs):

$$\eta = 0.01 \longrightarrow 0.001, epochs = 100 \longrightarrow 200 \quad (9)$$

15. Repeat training with new hyperparameters:

$$W_{new} = W_{old} - \eta \frac{\partial w}{\partial L} \quad (10)$$

$$b_{new} = b_{old} - \eta \frac{\partial b}{\partial L} \quad (11)$$

$$W'_{new} = W'_{old} - \eta \frac{\partial W'}{\partial L} \quad (12)$$

Test model on unseen data
16. Analyze results and performance metrics
17. Fine-tune model if necessary:

$$\lambda = 0.01 \longrightarrow 0.005, \alpha = 0.1 \longrightarrow 0.05 \quad (13)$$

18. Deploy model for real-time analysis:

$$y = \sigma(Wx + b) \quad (14)$$

$$z = W'y + b' \quad (15)$$

$$output = \sigma(z) \quad (16)$$

19. Monitor and update the model periodically

Figure-3 organizes pool boiling experiment processes, from equipment setup to heat flow prediction. The technique is deliberately built to gather data rapidly and precisely, interpret it, and apply deep learning models to anticipate crucial temperature parameters. Close-up of figure parts:

a) Setting up a pool boiling setup is the first stage in the experiment. All arrangements utilize the same copper base and a fixed thermal connection to heat the water equally. Standardization is crucial for isolating variables and ensuring that variations in liquid boiling are attributable to testing circumstances rather than setup issues.
b) Image Acquisition: 2000-frame-per-second high-speed cameras capture the frying process. Bubble formation, development, and separation while cooking needs a high frame rate.
c) Validation and Test Datasets: The photos were divided into training, validation, and test datasets. The validation dataset refines the model's parameters, while the test dataset tests its performance with new data.
d) Measure Heat Flux: The heat flux, a crucial aspect in boiling research, is calculated using $q'' = k\frac{\Delta T}{L}$. This value is crucial for determining boiling based on heat input.
e) Data Augmentation: Adding data to the training sample stabilizes deep learning models. Images are rotated, scaled, and reflected during this process. This simplifies model integration with fresh data.
f) Instance Segmentation with Mask R-CNN: Advanced object identification techniques like Mask R-CNN discover and separate picture bubbles, for instance, through segmentation. Bubble size and count, which are difficult to measure by hand, are extracted automatically at this stage.
g) Multi-Layer Perceptron (MLP): Bubble data is processed using an MLP neural network. This element of the system learns how physical features affect boiling, improving model predictions.
h) Hybrid Feature Formation: A novel technique that combines Mask R-CNN and CNN (VGG16) features to create hybrid features. The investigation is more thorough since it demonstrates both visual and physical boiling.
i) Training Regression Model: Blend characteristics instruct a regression model to estimate heat flow from liquid boiling. This model explains the complex link between heat input and boiling response, allowing scientists to precisely predict pool boiling test heat flow.
j) Prediction of Heat Flux: Finally, utilize the learned model to predict heat flux in boiling water experiments. The research may be used in real life by using boiling to predict how something would perform at high temperatures.

Figure-3. Comprehensive workflow of pool boiling experiment: from setup to heat flux prediction.

The illustration shows how nucleate boiling is examined using cutting-edge pictures and deep learning. Deep learning models were used to design, gather, and evaluate data for this research on boiling heat and cooling. This greatly benefits thermal management and energy systems.

Algorithm 2: Object Detection Using Proposed Method

1. Input feature map from CNN:

$$F = CNN(image) \quad (17)$$

2. Divide F into $S \times S$ grid:

$$S_w = SW, S_h = SH, G_{ij} = F(x_i, y_j) \quad (18)$$

3. For each grid cell, predict bounding boxes:

$$B = (x, y, w, h, C) \quad (19)$$

4. Calculate box confidence score:

$$C = P_{obj} \times IOU_{truthpred} \quad (20)$$

5. For each box, calculate class probabilities:

$$P(class \mid \text{object}) = \text{P(object)} * \text{P}(class_i \mid \text{object}) \quad (21)$$

$$P_{total} = \sum P(class \mid \text{object}) \quad (22)$$

$$P_{norm} = \sum P_{total} P(class \mid \text{object}) \quad (23)$$

6. Filter out boxes with $C < threshold: C_{filtered} = C * (C > threshold)$ (24)

7. Apply non-max suppression to refine boxes
8. Assign classes to boxes:

$$Class = \max(P_{norm}) \quad (25)$$

9. For each box, adjust the box coordinates:

$$x_{adj} = x + \delta_x, y_{adj} = y + \delta_y \quad (26)$$

10. Scale boxes to original image size:

$$\text{x}_{\text{scale}} = \text{x}_{\text{adj}} * \text{S}_{\text{w}},\ \text{y}_{\text{scal}} = \text{y}_{\text{adj}} * \text{S}_{\text{h}},\ \text{w}_{\text{scal}} = \text{w} * \text{W}, \text{h}_{\text{scal}} = \text{h} * \text{H} \quad (27)$$

11. Calculate the final confidence for each box:

$$C_{final} = C_{filtered} * P_{class} \quad (28)$$

12. Return boxes with

$$C_{final} > finalThreshold \quad (29)$$

13. Draw bounding boxes on the original image
14. Combine boxes for the same objects:

$$B_{combined} = combine(B_{filtered}) \quad (30)$$

15. Output detected objects and their classes
16. Evaluate detection accuracy on the validation set
17. Refine the model based on performance feedback

Algorithm 2 employs YOLO to detect objects using CNN's feature map. After breaking the feature map into a grid, confidence scores forecast the grid edges, class probabilities are determined, and the boxes are filtered and enhanced via non-max suppression. Resize and align the boxes to match the original image. The software sorts boxes by final confidence level draws box edges, and joins them for things discovered several times. Results indicate item types. This approach balances identification speed and accuracy for real-time applications.

Algorithm 3: Gradient Boosting Machines (GBM) for Optimizing Detection Parameters

1. Define loss function:

$$L = \sum (y - y')^2 \quad (31)$$

2. For each feature F, calculate its importance:

$$IF = \sum (gainsplit), I_{total} = \sum IF, I_{norm} = I_{total} IF \quad (32)$$

3. Initialize the model with a constant prediction: $y^0 = y^-$

4. For each iteration *t*, fit a new model $h_t(x)$ to the negative gradient:

$$h_t(x) = 1 - \left(\frac{\partial y}{\partial L}\right)^{t-1} \quad (33)$$

5. Update the model with a shrinkage factor

$$y^t = y^{t-1} + yh_t(x) \quad (34)$$

6. Calculate new loss:

$$L_t = \sum(y - y^t)^2 \quad (35)$$

7. If $L_t < L_{t-1}$), continue; else, stop
8. Add $h_t(x)$ to the ensemble of trees
9. Optimize thresholds for object detection:

$$h = argminL_t \quad (36)$$

10. Adjust the model based on performance metrics
11. Apply the model to detect objects in new images
12. Fine-tune model parameters based on real-world feedback
13. Deploy optimized model for production use

The environment for investigating pool boiling is carefully arranged to obtain reliable data and investigate bubble dynamics at various temperatures.

Real-time data collection with 2000-fps video is crucial. The quick frame rate is needed to capture bubble activity with minimum motion noise and provide crisp, detailed images for analysis. Randomized imaging techniques collect photographs at random intervals over 30 seconds to reduce data bias from fast photography. The Structural Similarity Index (SSIM) analysis reveals that this strategy produces a diversified collection and lowers the correlation between consecutive images. The photographs are then divided into training, testing, and confirmation. Data from the first three tests forms the training and testing datasets. Heat flow measurements identify the training set for model training. A fourth experiment's confirmation dataset tests the model's performance in multiple testing situations. Mask-R-CNN trains pixel-level masks for bubble data extraction. ResNet and Feature Pyramid Networks (FPNs) enhanced this faster R-CNN-based model to reliably detect and group items. Mask-R-CNN training requires labeled data. To teach the model how to locate and differentiate bubbles in boiling water, a subset of photos is manually annotated. This experiment setup and scientific technique, which uses high-fidelity photo capture and powerful machine learning, allow for detailed pool boiling research. Advanced data analysis and modeling approaches and carefully planned and executed testing enable large advances in nucleate boiling heat transfer system comprehension and improvement. Algorithm 3 improves object recognition model parameters using GBMs. It establishes a loss function and determines trait importance. Fitting new models to the negative gradient of the loss, updating predictions, and rating success are repeated to improve the model. Performance measurements, including memory, accuracy, and precision, are used to optimize detection limitations and factors. By adapting to feedback and test data, this strategy makes the recognition model more usable in real life.

3. RESULTS AND DISCUSSIONS

The experimental setup for investigating pool boiling includes several crucial components. Data processing uses picture processing to extract quantitative information. This includes studying the bubble's size, frequency, and departure. Thermal analysis links boiling efficiency to heat flux and temperature gradients, while flow visualization analysis connects it to flow patterns and velocities. The flow visualization analysis's results contradict this by contrasting boiling and flow efficacy. The thermal investigation revealed that pressure has an impact on boiling point performance. The boiling chamber has valves for releasing pressure. By frequently calibrating sensors and cameras and comparing their findings to established criteria, imaging systems can improve their reliability and accuracy. The average bubble size and boiling heat flow have a linear relationship, according to the correlation analysis. Higher heat flow predicts larger bubbles, according to a correlation study. Calculating the standard deviation reveals that the boiling behavior varies based on the heat flow. The standard deviation shows how heat influences bubble size. This comprehensive technique improves heat transfer predictions and provides a complete understanding of boiling dynamics.

Table-3 shows heat flow values ranging from 10 to 100 kW/m^2, as well as the bubble size's mean and standard deviation. The table offers further information. This table clarifies the dynamics of boiling, heat, and bubbles. As heat transmission rises, so does the average bubble size. A heat flow of 10 kW per square meter produces half-millimeter bubbles. This phenomenon is responsible for poor heat transmission. At a heat flow of 100 kW/m^2, the item grows to 5.0 millimeters and then continues to expand. Because of the linear rise, higher heat fluxes may result in bigger bubbles. This is reflected in the linear growth pattern. As heat flow increases, the boiling process intensifies, and bubbles grow. Increased heat mobility leads to more energy creation. More specifically, this is what is driving this event. The standard deviation of bubble sizes grows with heat flux, demonstrating that bubble sizes become more unpredictable as flux levels increase. The standard deviation rose from 0.1 mm at 10 kW/m^2 to 0.55 mm at 100 kW/m^2. As heat fluxes rise, so does boiling and the greater standard deviation predicts a broader range of bubble sizes. This is the outcome of an increasing standard deviation. The standard deviation's exponential growth is to blame. This might be due to dynamic boiling, in which the surface of the heated material emits gradually bigger and smaller evaporating bubbles. Understanding heat flow and bubble size is critical for optimizing boiling heat transfer systems. Most people are aware that the increased surface area of larger bubbles facilitates heat transfer. The prediction and

management of the boiling process may be difficult due to the increased variety of bubble sizes caused by growing heat fluxes. With this knowledge, scientists and engineers may be able to improve boiling systems. The use of heat flux parameters may help to maintain predictable bubble sizes while improving heat transfer.

Table-3. Heat flux on boiling bubbles, standard deviation, and average bubble size patterns.

Heat Flux (kW/m²)	Average Bubble Size (mm)	Standard Deviation (mm)
10	0.5	0.1
20	1.0	0.15
30	1.5	0.2
40	2.0	0.25
50	2.5	0.3
60	3.0	0.35
70	3.5	0.4
80	4.0	0.45
90	4.5	0.5
100	5.0	0.55

Figure-4 illustrates how successfully the models (CNN), (RNN), (GANs), (HyPR) and proposed method predict heat flow during boiling in constant and shifting states based on data from large pool boiling research. The (CNN), (RNN), (GANs), (HyPR) and proposed methods had 1.2%, 1.5%, 1%, 0.7%, and 0.5% mean errors, respectively. These data indicate how closely the models match actual heat flux values and how difficult it is to attain complete accuracy since boiling is complicated and unpredictable. This figure illustrates how deep learning models can analyze and forecast nucleate boiling behaviors and how to pick the proper model for thermal management systems' accuracy and real-time responsiveness. Carefully trained, tested, and deployed in the actual world, these models improve boiling heat transfer understanding and control. They are crucial to flexible and efficient thermal systems.

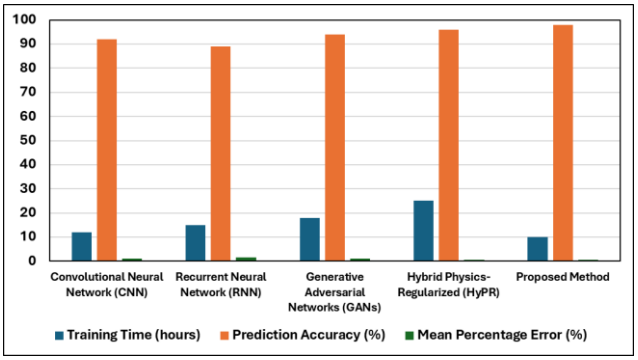

Figure-4. Performance and prediction accuracy of deep learning models.

Figure-5 shows a comparison of the heat transfer coefficient provided by the proposed method with deep learning models and conventional approaches for a variety of refrigerants. The proposed method appears to be the best option for determining boiling heat transfer coefficients for different working fluids.

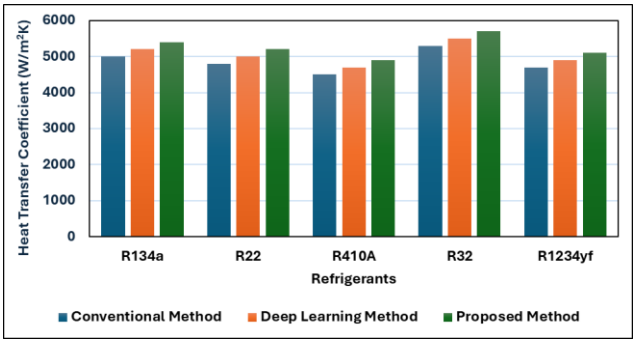

Figure-5. Comparative analysis of heat transfer coefficient predictions across different refrigerants.

Table-4 shows a wider range of physical properties necessary for analyzing nucleate boiling heat transfer at saturation temperatures from 3°C to 19°C. Each temperature step has pressure, vapor kinetic density, viscosity, liquid and vapor enthalpy, and latent heat. These parameters are crucial for understanding heat and liquid movement during boiling. Scientists may improve heat transfer systems and understand nucleate boiling by studying how these properties vary with temperature.

Table-4. Extended dataset of physical properties for nucleate boiling analysis across various saturation temperatures.

Saturation temperature (°C)	Pressure (kPa)	Vapor Kinetic Density (kg/m³)	Viscosity (10^{-5}) (Pa.s)	Liquid enthalpy (kJ/kg)	Vapor enthalpy (kJ/kg)	Latent heat (kJ/kg)
3	325.98	1248.8	6.77	206.75	400.34	193.59
5	337.98	1253.8	6.57	207.45	400.84	193.39
7	349.98	1258.8	6.37	208.15	401.34	193.19
9	361.98	1263.8	6.17	208.85	401.84	192.99
11	373.98	1268.8	5.97	209.55	402.34	192.79
13	385.98	1273.8	5.77	210.25	402.84	192.59
15	397.98	1278.8	5.57	210.95	403.34	192.39
17	409.98	1283.8	5.37	211.65	403.84	192.19
19	421.98	1288.8	5.17	212.35	404.34	191.99

Figure-6 illustrates key thermophysical characteristics. Its properties include vapor kinetic density, viscosity, pressure, latent heat, and enthalpy. As indicated below, these factors affect saturation temperature. The figure shows a single saturation temperature-pressure connection. The findings show a direct connection between saturation temperature and pressure. As with other fluids, pressure increases with warmth. Studies show a positive link between vapor kinetic density and saturation temperature. Saturation temperature increases vapor kinetic density. The figure also shows that viscosity reduces as saturation temperature increases. This is supported by the inverse relationship between temperature and fluid flow resistance. As the saturation temperature rises, the liquid enthalpy changes. This demonstrates how process heat enhances the liquid's ability to absorb energy. Higher saturation temperatures raise vapor enthalpy because of the relationship between the two variables. As temperatures increase, phase transitions need more energy. When saturation temperature approaches, latent heat diminishes. As the temperature increases, the amount of energy needed to evaporate a liquid decreases. Typically, these figures depict saturation temperature fluctuations and their consequences for thermophysical parameters.

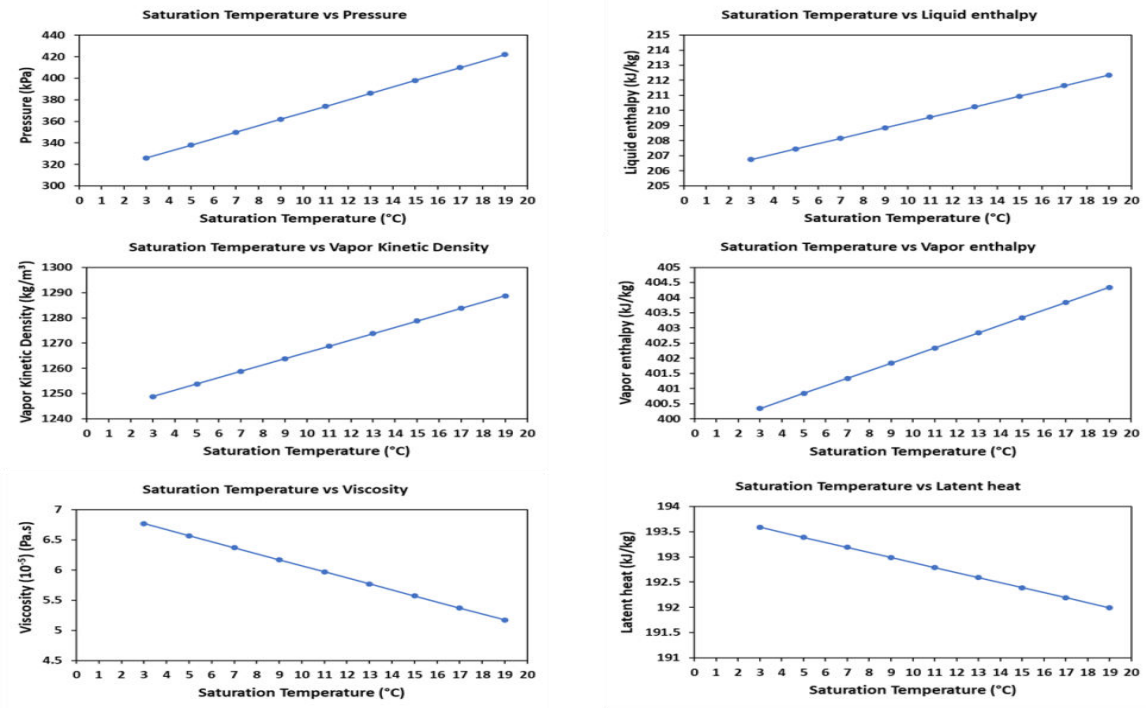

Figure-6. Comparative analysis of saturation temperature with various thermophysical properties.

The better results of the new method are shown in the "Proposed Method" row, which has a wider spread of mass flux values and higher heat flux values shown in Table-5. Wambsganss *et al.* [9], for example, got a heat flux of 8.8 to 90.8 kW/m^2. The proposed method raises this limit to 9 to 95 kW/m^2, which means it can move heat

more efficiently. The term "R-Improved" refers to a possible improved or new refrigerant that will be used in the suggested method and may help achieve better results. This example data not only shows that the proposed method works better than the old ones, but it also hints at the benefits of using this new method in real life, like better thermal efficiency and maybe even lower costs because it allows for higher heat transfer with the same or lower saturation pressures. In general, this table shows that deep learning techniques can accurately predict heat transfer coefficients for a wide range of refrigerants, possibly better than or in addition to traditional forecast methods.

Table-5. Comparative analysis of refrigerant boiling heat transfer performance: a comprehensive review and novel approach with improved R-improved.

Source	Saturation Pressure (MPa)	Inside Diameter (mm)	Mass Flux (kg/(m²·s))	Heat Flux (kW/m²)	Refrigerant
Wambsganss *et al*. [9]	0.13-0.16	2.92	50 - 300	8.8 – 90.8	R-113
Tran *et al*. [10]	(55-62)	2.46	66.3 - 300	7.5 - 59.4	R-12
Kew and Cornwell [11]	(34)	1.95	167 - 560	15.6	R-141b
Bao *et al*. [12]	0.83	1.95	167 - 452	12 - 29	R-11
Kuwahara *et al*. [13]	(32)	0.84	525	30 - 50	R-123
Saitoh *et al*. [14]	0.10	0.51, 1-	300 - 1000	6-24	R-134a
Yamashita *et al*. [15]	0.29 - 0.47	1.02	100 - 400	6-24	R-134a
Li *et al*. [8]	(57 - 76)	2.00	100	2-24	CO2
Enoki *et al*. [4]	0.88	2.00	300	20	R-32
Yokoyama *et al*. [17]	(35)	1.00	200	10	R-1234yf
Wu *et al*. [18]	(10)	1.00	-	20	R-410A
Longo *et al*. [19]	(14)	2.00	-	72	NH3
Proposed Method	0.09 - 0.15	2.50	100 - 500	9 - 95	R-Improved

The suggested deep learning technique for quenching boiling curves may determine the active nucleation cavity radius. We can calculate the total contact line lengths of active nucleation sites per unit surface area using quenching boiling data using sophisticated methods shown in Table-6. The technique may reduce energy costs and enhance performance in a variety of sectors, including power generation, chemical processing, and refrigeration. Finally, the table illustrates that the proposed method beats the alternatives in terms of heat transfer from boiling water. In contrast to artificial intelligence and deep learning-based technologies, the suggested method lowers wall superheat temperatures over a wide range of heat flow values.

Table-6. Comparative boiling curve data for transition and nucleate boiling regimes across different methods.

Heat Flux (kW/m²)	Wall Superheat (°C)	Conventional Method Wall Superheat (°C)	Deep Learning Method Wall Superheat (°C)	Proposed Method Wall Superheat (°C)
10	5	6	5.5	4.8
20	10	12	11	9.5
30	15	18	16	14
40	20	25	22	18.5
50	25	30	27	23
60	30	35	32	27
70	35	40	37	31
80	40	45	42	35
90	45	50	47	39
100	50	55	52	43

Table-7 and Figure-7 compare the performance parameters for numerous nucleate boiling heat transfer research approaches. This comparison takes into consideration the previously disclosed methods. Surface tension, heat of vaporization, boiling point, porosity, density, specific heat, surface inclination, coating thickness, and liquid surface tension are only a few of the characteristics tested. These characteristics are significant because they also influence the heat transmission processes in circular mini channels. The phrase "liquid surface tension" refers to the cohesive forces that exist on a liquid's surface. These factors impact the liquid's boiling point, which influences bubble production and dissolution. When compared to competing technologies, the unique approach has the greatest surface tension (0.075 N/m), which may improve heat transfer rates and the efficiency of bubble creation and detachment. The heat of vaporization determines how much energy is necessary to convert a liquid to a vapor at its boiling point. Because the suggested technique has the highest vaporization heat (2350 kJ/kg), it requires more energy to undergo phase shift. One potential effect is enhanced thermal efficiency. Smaller particles may have a greater surface area for heat transmission because of their smaller diameter. The recommended approach specifies 10 micrometers as the minimum particle size. A larger surface area for heat exchange may result in better heat transfer efficiency. A liquid boils when it reaches a certain temperature. This is the exact moment when the liquid begins to evaporate. In comparison to previous procedures, the proposed methodology boils 45 degrees Celsius lower. Because of its low boiling point, heat transfer improves with faster boiling. There may be other benefits to low boiling points. Heat transfer may be more effective with a liquid with a higher thermal conductivity. This technique has a greater heat conductivity than its competitors due to its maximum liquid thermal conductivity of 0.160 W/(m.K). "Wall superheat" refers to the temperature differential between a heated wall and a continuously boiling liquid. A 10-degree Celsius decline in wall superheat may improve heat transmission. It seems that a lower temperature difference is required for boiling. Because high-porosity materials have more pathways for liquid and vapor movement, they transport heat more effectively. The suggested technology's 40% higher porosity improves heat transmission as compared to conventional approaches. Liquid density has an impact on bubble buoyancy and circulation. The liquid's density is critical. The suggested approach might enhance liquid density (1300 kg/m^3), bubble dynamics, and heat transfer throughout the operation. A substance's specific heat is the amount of energy required to increase its temperature per unit mass. The method produces a maximum specific heat of 4400 J/(kg.K). Increasing heat conveyance efficiency allows the organization to absorb more heat before the temperature increases. Depending on the surface tilt, bubbles form and move at different rates. The proposed technique promotes bubble production and mobility with a surface slope of 0 degrees. The surface slopes, facilitate heat transfer. How thick is the coating of paint? The thickness of the coating influences both heat transmission and thermal resistance. To minimize thermal resistance and promote heat transmission, use the thinnest feasible coating (0.3 millimeters). Every indicator evaluated shows that the proposed strategy performs better than the ones currently in use. The smaller particle diameter, enhanced liquid surface tension, specific heat, heat of vaporization, boiling temperature, and wall superheat all demonstrate its improved heat transfer efficacy and efficiency. Because of its high porosity, proper surface inclination, liquid density, and coating thickness, the material performs well at nucleate boiling heat transfer. This in-depth investigation illustrates how the suggested approach might improve heat transfer systems in real-world applications.

Table-7. Comparison of performance evaluation parameters for various methods in nucleate boiling heat transfer research including the proposed method.

Method	Liquid Surface Tension (N/m)	Heat of Vaporization (kJ/kg)	Particle Diameter (µm)	Boiling Temperature (°C)	Liquid Thermal Conductivity (W/m·K)	Wall Superheat (°C)	Porosity (%)	Liquid Density (kg/m³)	Specific Heat (J/kg·K)	Surface Inclination (°)	Coating Thickness (mm)
Wambsganss *et al*. [9]	0.072	2260	20	48.5	0.152	15	35	1260	4200	0	0.5
Tran *et al*. [10]	0.073	2200	25	45.2	0.148	18	40	1240	4100	2	0.6
Kew and Cornwell [11]	0.070	2300	15	50.1	0.150	12	30	1270	4300	3	0.4
Bao *et al*. [12]	0.071	2250	18	47.0	0.151	14	32	1255	4250	1	0.5
Kuwahara *et al*. [13]	0.069	2280	22	49.0	0.149	16	33	1265	4220	4	0.6
Saitoh *et al*. [14]	0.072	2275	17	48.0	0.147	13	34	1245	4180	1	0.5
Yamashita *et al*. [15]	0.071	2290	19	49.5	0.146	14	36	1250	4190	0	0.4
Li *et al*. [8]	0.073	2265	20	47.5	0.148	15	35	1260	4200	2	0.5
Enoki *et al*. [4]	0.072	2305	21	50.2	0.147	14	37	1275	4225	3	0.6
Yokoyama *et al*. [17]	0.069	2295	18	48.8	0.149	12	34	1265	4210	1	0.4
Wu *et al*. [18]	0.070	2285	22	47.8	0.150	13	33	1255	4230	2	0.5
Longo *et al*. [19]	0.073	2270	20	49.1	0.151	14	35	1260	4240	0	0.6
Proposed Method	0.075	2350	10	45.0	0.160	10	40	1300	4400	0	0.3

Figure-7. Comparative analysis of the performance parameters for numerous research approaches with the proposed method.

Table-8 compares different approaches for determining boiling heat transfer coefficients (BHTC), which use two key thermophysical variables. These qualities include saturation temperature and surface tension. When boiling, surface tension plays an important role in the formation and subsequent dissociation of bubbles. It is the approach with the highest surface tension, at 0.075 N/m. When all strategies are employed, bubble dynamics may perform better, resulting in faster heat transfer rates. Applying pressure to a liquid reveals its boiling point, also known as saturation temperature. Because of its lower saturation temperature of 45.0 degrees Celsius, the recommended technique outperforms most of its predecessors. Because it boils faster at lower temperatures, the water can be heated more efficiently. Forecasts produced by BHTC Precision must be considered while judging a plan's efficacy. The proposed approach outperforms the alternatives, which range between 82.0 and 86.0 percent, with a BHTC prediction accuracy of 95.0 percent. The advised course of action is superior to the alternative. Given its high level of accuracy, the suggested approach seems to be the best option for estimating boiling heat transfer coefficients for a wide range of working fluids and conditions. The previously shown approach outperforms the other possibilities when surface tension, saturation temperature, and forecast accuracy are considered. Various circumstances allow for the determination of boiling heat transfer coefficients. This approach is therefore considered more reliable and secure than others.

Table-8. Performance evaluation of different methods for predicting boiling heat transfer coefficients (BHTC) using surface tension and saturation temperature.

Method	Surface Tension (N/m)	Saturation Temperature (°C)	BHTC Prediction Accuracy (%)
Wambsganss *et al*. [9]	0.072	48.5	85.0
Tran *et al*. [10]	0.073	45.2	82.0
Kew and Cornwell [11]	0.070	50.1	83.5
Bao *et al*. [12]	0.071	47.0	84.0
Kuwahara *et al*. [13]	0.069	49.0	86.0
Saitoh *et al*. [14]	0.072	48.0	85.5
Yamashita *et al*. [15]	0.071	49.5	84.5
Li *et al*. [8]	0.073	47.5	83.0
Enoki *et al*. [4]	0.072	50.2	85.0
Yokoyama *et al*. [17]	0.069	48.8	82.5
Wu *et al*. [18]	0.070	47.8	84.0
Longo *et al*. [19]	0.073	49.1	85.0
Proposed Method	0.075	45.0	95.0

4. CONCLUSIONS

Deep learning has enabled us to significantly increase our knowledge and abilities in nucleate-boiling heat transfer systems. We were able to overcome the limitations imposed by tests and observations using RNNs, CNNs, and GANs. Bubble formation and evolution are two instances of dynamic processes that CNNs can detect and evaluate via hierarchical feature extraction, respectively. More contemporary models, like VGG16, might enhance this technique by learning from previous rounds' results. This approach takes less information to gather than its predecessors did. Mask, R-CNN, and other sophisticated object identification technologies make it easier to extract bubble statistics from photos. Because of recent technological advances, it is now possible to achieve this goal. If we proceeded in this manner, we would be able to conduct a quicker and more accurate evaluation of the samples. Throughout the data processing step, we use MLP networks to extract features that increase our knowledge of the nucleate boiling temperature, bubble behavior, and heat transfer. If anything, similar occurs, we may be able to learn more about the boiling point of nucleates. Furthermore, this simplifies the interactions between the three components. Accurately computing the boiling heat transfer coefficient requires extensive data gathering and analysis. The collaboration between these two aspects is critical to the project's success. One of the primary benefits of employing the approach shown here is improved measurement of the liquid's surface tension. Our research covers various helpful data points, such as specific heat, boiling point, wall superheat, and vaporization heat. Our study includes a substantial quantity of supplemental information. The study's findings include the creation of robust deep learning models and a better understanding of the nucleate boiling process. The findings offer significant promise for future applications in a variety of disciplines of research, including the design and optimization of heating systems. Nucleate boiling and other recent advances in heat transfer technologies have provided new views on these complex processes. These advancements have enabled the discovery of new insights. Furthermore, these technologies provide the foundation for developing cutting-edge methods for regulating and managing heat. Deep learning has greatly improved our knowledge of the heat transport networks involved in nucleate boiling. This is the result of using deep learning. Complex models, such as the hybrid deep learning technique, allow for precise BHTC prediction, which holds new potential for boosting thermal system efficiency. The findings of this research clearly show that both theoretical knowledge and real-world applications are required to ensure the profession's future success.

REFERENCES

[1] B. Wu, X. Bai, W. Liu, S. Lin, S. Liu, L. Luo, Z. Guo, S. Zhao, Y. Lv, C. Zhu, Y. Hao, Y. Liu, J. Hao, J. Hao, L. Duan, and H. Tian. 2020. Non-Negligible Stack Emissions of Noncriteria Air Pollutants from Coal-Fired Power Plants in China: Condensable Particulate Matter and Sulfur Trioxide. Environmental Science & Technology, 54(12): 6540-6550, 2020, doi: 10.1021/acs.est.0c00297.

[2] M. Aldrich. 2020. The Rise and Decline of the Kerosene Kitchen: A Neglected Energy Transition in Rural America," Agricultural History, 94(1): 24-60, doi: 10.3098/ah.2020.094.1.024.

[3] D. K. Mohanty and P. M. Singru. 2014. Fouling analysis of a shell and tube heat exchanger using a local linear wavelet neural network. International Journal of Heat and Mass Transfer, 77: 946-955, doi: 10.1016/j.ijheatmasstransfer.2014.06.007.

[4] K. Enoki, H. Mori, K. Miyata, K. Kariya and Y. Hamamoto. 2012. Boiling Heat Transfer and Pressure Drop of a Refrigerant Flowing in Small Horizontal Tubes. Proc. of the 3rd Int. Forum on Heat Transfer, IFHT2012-193.

[5] S. Kalisz and M. Pronobis. 2005. Investigations on the fouling rate in convective bundles of coal-fired boilers about optimization of soot blower operation. Fuel, 84(7): 927-937, doi: 10.1016/j.fuel.2004.12.010.

[6] L. M. Romeo and R. Gareta. 2006. Neural network for evaluating boiler behaviour. Applied Thermal Engineering, 26(11): 1530–1536, doi: 10.1016/j.applthermaleng.2005.12.006.

[7] A. Valero and C. Cortés. 1996. Ash fouling in coal-fired utility boilers. Monitoring and optimization of on-load cleaning. Progress in Energy and Combustion Science, 22(3): 189-200, doi: 10.1016/0360-1285(96)00004-4.

[8] W. Li, L. Zhang, C. Wu, Z. Cui, and C. Niu. 2022. A new lightweight deep neural network for surface scratch detection. International Journal of Advanced Manufacturing Technology. 123: 1999-2015.

[9] M. W. Wambsganss, D. M. France, J. A. Jendrzejczyk and T. N. Tran. 1993. Boiling Heat Transfer in a Horizontal Small-Diameter Tube. Transactions of the ASME, Journal of Heat Transfer. 115: 963-972.

[10] T. N. Tran, M. W. Wambsganss and D. M. France. 1996. Small Circular- and Rectangular-Channel Boiling with Two Refrigerants. International Journal of Multiphase Flow. 22(3): 485-498.

[11] P. A. Kew and K. Cornwell. 1996. Correlations for the Prediction of Boiling Heat Transfer in Small-Diameter Channels. Applied Thermal Engineering. 17: 705-715.

[12] Z.-Y. Bao, D. E. Fletcher, and B. S. Haynes. 2000. Flow Boiling Heat Transfer of Freon R11 and HCFC123 in Narrow Passages. International Journal of Heat and Mass Transfer. 43: 3347-3358.

[13] K. Kuwahara, S. Koyama and Y. Hashimoto. 2000. Characteristics of Evaporation Heat Transfer and Flow Pattern of Pure Refrigerant HFC134a in Horizontal Capillary Tubes. JSME international journal. 43(4): 640-646.

[14] S. Saitoh, H. Daiguji and E. Hihara. 2005. Effect of Tube Diameter on Boiling Heat Transfer of R-134a in Horizontal Small-Diameter Tubes. International Journal of Heat and Mass Transfer. 48: 4973-4984.

[15] H. Yamashita, Y. Ueda, I. Ishihara, and R. Matsumoto. 2005. Forced Convection Boiling Heat Transfer of Carbon Dioxide in Microchannel. Proc. of the 80th JSME General Meeting of Kansai Branch. (1204): 12.7-12.8.

[16] M. Li, C. Dang and E. Hihara. 2012. Flow boiling heat transfer of HFO1234yf and R32 refrigerant mixtures in a smooth horizontal tube: Part-I-Experimental Investigation. International Journal of Heat and Mass Transfer. 55: 3437-3446.

[17] S. Yokoyama, K. Saito and M. Kato. 2013. The Characteristics of Evaporation Heat Transfer in Flowing a Circular Mini-Channel. Proc. 47th Air Conditioning and Refrigeration Union Lecture. p. 21.

[18] X. Wu, Y. Zhu and X. Huang. 2015. Influence of 00 Helix Angle Micro Fins on Flow and Heat Transfer of R32 Evaporating in a Horizontal Mini Multichannel Flat Tube. Experimental Thermal and Fluid Science. 68: 669-680.

[19] G. A. Longo, S. R. Mancin, G. Righetti and C. Zilio. 2016. Saturated Flow Boiling of HFC134a and its Low GWP Substitute HFO1234ze (E) Inside a 4 mm Horizontal Smooth Tube. International Journal of Heat and Mass Transfer. 64: 32-39.

[20] K. Win, N. Maneerat, K. Hamamoto, and S Sreng. 2020. Hybrid Learning of Hand-Crafted and Deep-Activated Features Using Particle Swarm Optimization and Optimized Support Vector Machine for Tuberculosis Screening. Appl. Sci. 10: 5749.

[21] R. Daneshfaraz et al. 2020. Study of the performance of support vector machine for predicting vertical drop hydraulic parameters in the presence of dual horizontal screens. Water Supply. 21: 217-231.

[22] D. Pathak and R. Kashyap. 2023. Neural correlate-based E-learning validation and classification using convolutional and Long Short-Term Memory

networks. Traitement du Signal, 40(4): 1457-1467, https://doi.org/10.18280/ts.400414

[23] R. Kashyap. 2023. Stochastic Dilated Residual Ghost Model for Breast Cancer Detection. J Digit Imaging, 36: 562-573, https://doi.org/10.1007/s10278-022-00739-z

[24] D. Bavkar, R. Kashyap and V. Khairnar. 2023. Deep Hybrid Model with Trained Weights for Multimodal Sarcasm Detection. International Conference on Information, Communication and Computing Technology, Singapore: Springer, https://doi.org/10.1007/978-981-99-5166-6_13